Experimental demonstration of spinor slow light

Meng-Jung Lee[a], Julius Ruseckas[b], Chin-Yuan Lee[a], Viačeslav Kudriašov[b], Kao-Fang Chang[a], Hung-Wen Cho[a], Gediminas Juzeliūnas[b], and Ite A. Yu[a]
[a]Department of Physics and Frontier Research Center on Fundamental and Applied Sciences of Matters, National Tsing Hua University, Hsinchu 30013, Taiwan;
[b]Institute of Theoretical Physics and Astronomy, Vilnius University, A. Goštauto 12, Vilnius 01108, Lithuania

ABSTRACT

Over the last decade there has been a continuing interest in slow and stored light based on the electromagnetically induced transparency (EIT) effect, because of their potential applications in quantum information manipulation. However, previous experimental works all dealt with the single-component slow light which cannot be employed as a qubit. In this work, we report the first experimental demonstration of two-component or spinor slow light (SSL) using a double tripod (DT) atom-light coupling scheme. The oscillations between the two components, similar to the Rabi oscillation of a two-level system or a qubit, were observed. Single-photon SSL can be considered as two-color qubits. We experimentally demonstrated a possible application of the DT scheme as quantum memory and quantum rotator for the two-color qubits. This work opens up a new direction in the slow light research.

Keywords: EIT, slow light, stored light, spinor slow light, two-color qubit, quantum memory, quantum rotator.

1. INTRODUCTION

Based on the effect of electromagnetically induced transparency (EIT)[1-3], the developments of slow light[4-8], storage of light[9-17], and stationary light pulses[18-21] have attracted great attention. The slow light as well as the stationary light pulse greatly enhances the interaction time between light and matter and, therefore, makes nonlinear optical processes achieve significant efficiencies even at low-light or single-photon level[22-35]. The storage of light provides a method of coherent transfer of wave functions between photons and atoms[36-43] and has the great potential in applications of quantum memory. These developments have made important impacts to quantum information science and can lead to the applications in manipulation of quantum information.

Utilizing a double tripod (DT) atom-light coupling scheme[44-47], we experimentally demonstrated the two-component or spinor slow light (SSL)[48]. The DT scheme is a combination of two single-tripod schemes[49-53], but its physics is more abundant due to the interaction between the two components of light coupled with two atomic coherences. SSL exhibits a number of additional distinct features, such as formation of the quasi-particles characterized by the Dirac spectra[44,45] or oscillations[45,46] between the two components. Furthermore, the SSL can be exploited in designing novel photonic devices, e.g. interferometers for sensitive measurements and quantum memory/rotator for two color qubits, which will be discussed later in this article.

This article is organized as follows. The theoretical model of SSL formed in the DT system is given in Section 2. In the next section, we illustrate the experimental setup. Then we show the experimental results and discuss them in Section 4. Finally, the article finishes with a conclusion.

2. THEORETICAL MODEL

The DT level scheme consists of three atomic ground states $|0\rangle$, $|1\rangle$ and $|2\rangle$ and two excited states $|A\rangle$ and $|B\rangle$, as depicted in Fig. 1. One probe field (with the Rabi frequency ε_A) and two coupling fields (with the Rabi frequencies Ω_{A1} and Ω_{A2}) drive the transitions from $|0\rangle$, $|1\rangle$ and $|2\rangle$ to $|A\rangle$, respectively, to form the first tripod configuration. Another probe field (with the Rabi frequency ε_B) and the other two coupling fields (with the Rabi frequencies Ω_{B1} and Ω_{B2}) drive the

*yu@phys.nthu.edu.tw; phone +886-3574-2539; fax +886-3572-3052; http://atomcool.phys.nthu.edu.tw/

Slow Light, Fast Light, and Opto-Atomic Precision Metrology IX, edited by Selim M. Shahriar, Jacob Scheuer, Proc. of SPIE Vol. 9763, 97630P · © 2016 SPIE
CCC code: 0277-786X/16/$18 · doi: 10.1117/12.2220197

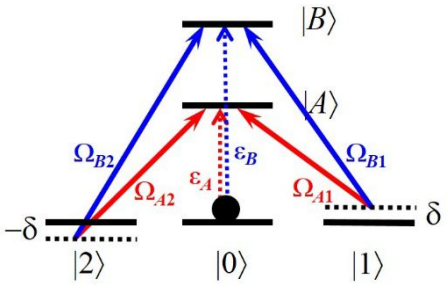

Figure 1. Relevant energy levels and laser excitations in the double-tripod system. ε_A and ε_B represent the probe fields; Ω_{A1}, Ω_{A2}, Ω_{B1} and Ω_{B2} indicate the coupling fields; δ (or $-\delta$) is the two-photon detuning, i.e. the probe detuning subtracts the coupling detuning, with respect to the Raman transition between $|0\rangle$ and $|1\rangle$ (or $|0\rangle$ and $|2\rangle$). In the experiment utilizing laser-cooled ^{87}Rb atoms, $|0\rangle$, $|1\rangle$, $|2\rangle$, $|A\rangle$ and $|B\rangle$ represent the Zeeman states of $|5S_{1/2},F=2,m=2\rangle$, $|5S_{1/2},F=2,m=0\rangle$, $|5S_{1/2},F=1,m=0\rangle$, $|5P_{1/2},F=2,m=1\rangle$ and $|5P_{3/2},F=2,m=1\rangle$, respectively. The wavelength of ε_A, Ω_{A1} and Ω_{A2} is 795 nm and that of ε_B, Ω_{B1} and Ω_{B2} is 780 nm. The spontaneous decay rate Γ of the excited states $|A\rangle$ and $|B\rangle$ is approximately equal to $2\pi\times6$ MHz.

transitions from the same ground states to $|B\rangle$ to form the second tripod configuration. The dynamics of the two probe fields and atomic coherences can be described by the following Maxwell-Bloch equations:

$$\frac{1}{c}\frac{\partial}{\partial t}\begin{bmatrix}\varepsilon_A\\ \varepsilon_B\end{bmatrix}+\frac{\partial}{\partial z}\begin{bmatrix}\varepsilon_A\\ \varepsilon_B\end{bmatrix}=i\frac{\alpha\Gamma}{2L}\begin{bmatrix}\rho_A\\ \rho_B\end{bmatrix}, \tag{1}$$

$$\frac{\partial}{\partial t}\begin{bmatrix}\rho_A\\ \rho_B\end{bmatrix}=\frac{i}{2}\begin{bmatrix}\varepsilon_A\\ \varepsilon_B\end{bmatrix}+\frac{i}{2}\begin{bmatrix}\Omega_{A1} & \Omega_{A2}\\ \Omega_{B1} & \Omega_{B2}\end{bmatrix}\begin{bmatrix}\rho_1\\ \rho_2\end{bmatrix}-\frac{\Gamma}{2}\begin{bmatrix}\rho_A\\ \rho_B\end{bmatrix}, \tag{2}$$

$$\frac{\partial}{\partial t}\begin{bmatrix}\rho_1\\ \rho_2\end{bmatrix}=\frac{i}{2}\begin{bmatrix}\Omega_{A1}^* & \Omega_{B1}^*\\ \Omega_{A2}^* & \Omega_{B2}^*\end{bmatrix}\begin{bmatrix}\rho_A\\ \rho_B\end{bmatrix}+\begin{bmatrix}i\delta & 0\\ 0 & -i\delta\end{bmatrix}\begin{bmatrix}\rho_1\\ \rho_2\end{bmatrix}+\begin{bmatrix}-\gamma & 0\\ 0 & -\gamma\end{bmatrix}\begin{bmatrix}\rho_1\\ \rho_2\end{bmatrix}, \tag{3}$$

where ρ_A (or ρ_B) is the coherence of the probe transition $|0\rangle\rightarrow|A\rangle$ (or $|0\rangle\rightarrow|B\rangle$), ρ_1 (or ρ_2) is the atomic ground-state coherence between $|0\rangle$ and $|1\rangle$ (or between $|0\rangle$ and $|2\rangle$), Γ is the spontaneous decay rate of the excited states $|A\rangle$ and $|B\rangle$, α and L are the optical density (OD) and length of the medium, δ or $-\delta$ is the two-photon detuning, and γ is the dephasing rate of the atomic coherences ρ_1 and ρ_2. The probe fields are assumed to be much weaker than the coupling fields such that one can treat the probe fields as a perturbation. All atomic population is in the ground state $|0\rangle$. The fast-oscillation exponential factors associating with center frequencies and the wave vectors have been eliminated from the equations, and only slowly-varying amplitudes are retained.

We focus on the case where the complex Rabi frequencies of the four coupling fields have the same amplitude of Ω. Thus, the complex Rabi frequency of the nth coupling field is $\Omega_n=\Omega e^{i\theta_n}$ with $n = A1$, $A2$, $B1$ or $B2$, where θ_n is the phase of coupling field. We define $\theta\equiv(\theta_{A1}-\theta_{A2})-(\theta_{B1}-\theta_{B2})$ to be a relative phase among the four coupling fields. To simplify the derivation, we take $\gamma=0$. For the continuous waves, Eqs. (1)-(3) reduce to

$$\frac{\partial}{\partial z}\begin{bmatrix}\varepsilon_A\\ \varepsilon_B\end{bmatrix}=i\frac{\alpha\Gamma}{2L}\begin{bmatrix}\rho_A\\ \rho_B\end{bmatrix}, \tag{4}$$

$$0=\frac{i}{2}\begin{bmatrix}\varepsilon_A\\ \varepsilon_B\end{bmatrix}+\frac{i}{2}\begin{bmatrix}e^{i\theta/2}\Omega & \Omega\\ \Omega & e^{i\theta/2}\Omega\end{bmatrix}\begin{bmatrix}\rho_1\\ \rho_2\end{bmatrix}-\frac{\Gamma}{2}\begin{bmatrix}\rho_A\\ \rho_B\end{bmatrix}, \tag{5}$$

$$0=\frac{i}{2}\begin{bmatrix}e^{-i\theta/2}\Omega & \Omega\\ \Omega & e^{-i\theta/2}\Omega\end{bmatrix}\begin{bmatrix}\rho_A\\ \rho_B\end{bmatrix}+\begin{bmatrix}i\delta & 0\\ 0 & -i\delta\end{bmatrix}\begin{bmatrix}\rho_1\\ \rho_2\end{bmatrix}. \tag{6}$$

Here we set the phases of individual coupling fields $(\theta_{A1}, \theta_{A2}, \theta_{B1}, \theta_{B2}) = (\theta/2, 0, 0, \theta/2)$ such that their relative phase is θ. Other combinations, such as $(\theta/2, -\theta/2, 0, 0)$, $(\theta, 0, 0, 0)$, $(0, 0, 0, \theta)$, etc., can also achieve the same result below. To

derive the solution of the above equations, we first make use of Eqs. (5) and (6) to eliminate (ρ_1, ρ_2) and subsequently to express (ρ_A, ρ_B) in terms of (ε_A, ε_B) in Eq. (4). Thus, Eq. (4) becomes

$$\frac{\partial}{\partial z}\begin{bmatrix}\varepsilon_A\\ \varepsilon_B\end{bmatrix}=-\frac{\alpha}{2L}\frac{1}{1+\beta^2}\begin{bmatrix}1 & \beta\\ -\beta & 1\end{bmatrix}\begin{bmatrix}\varepsilon_A\\ \varepsilon_B\end{bmatrix},\ \text{where}\ \beta\equiv\frac{\Omega^2\sin(\theta/2)}{\delta\Gamma}. \tag{7}$$

The matrix on the right-hand side of the above equation can be diagonalized by transforming the two probe fields (ε_A, ε_B) to new variables (ε_a, ε_b) via a unitary transformation

$$\begin{bmatrix}\varepsilon_a\\ \varepsilon_b\end{bmatrix}=\frac{1}{\sqrt{2}}\begin{bmatrix}1 & i\\ i & 1\end{bmatrix}\begin{bmatrix}\varepsilon_A\\ \varepsilon_B\end{bmatrix}. \tag{8}$$

The transformed fields ε_a and ε_b represent the two normal modes inside the medium. After the diagonalization of the matrix in Eq. (7), the solution of (ε_a, ε_b) is easily obtained. We transform the solution of (ε_a, ε_b) to that of (ε_A, ε_B) given by

$$\begin{bmatrix}\varepsilon_A(L)\\ \varepsilon_B(L)\end{bmatrix}=\exp\left(-\frac{\alpha}{2}\frac{1}{1+\beta^2}\right)\begin{bmatrix}\cos\left(\frac{\alpha}{2}\frac{\beta}{1+\beta^2}\right) & -\sin\left(\frac{\alpha}{2}\frac{\beta}{1+\beta^2}\right)\\ \sin\left(\frac{\alpha}{2}\frac{\beta}{1+\beta^2}\right) & \cos\left(\frac{\alpha}{2}\frac{\beta}{1+\beta^2}\right)\end{bmatrix}\begin{bmatrix}\varepsilon_A(0)\\ \varepsilon_B(0)\end{bmatrix}. \tag{9}$$

For $\beta \gg 1$ or $\Omega^2\sin(\theta/2) \gg \delta\Gamma$, i.e. the two-photon detuning is small as compared with the coupling Rabi frequency (the common situation in the EIT experiments), the solution simplifies to

$$\begin{bmatrix}\varepsilon_A(L)\\ \varepsilon_B(L)\end{bmatrix}=\exp\left(-\frac{2\phi^2}{\alpha}\right)\begin{bmatrix}\cos\phi & -\sin\phi\\ \sin\phi & \cos\phi\end{bmatrix}\begin{bmatrix}\varepsilon_A(0)\\ \varepsilon_B(0)\end{bmatrix},\ \text{where}\ \phi=\frac{\alpha}{2}\frac{\delta\Gamma}{\Omega^2\sin(\theta/2)}. \tag{10}$$

As only one probe field is present at the input, e.g. $\varepsilon_A(0) = 1$ and $\varepsilon_B(0) = 0$, the transmissions of the two output probes are given by

$$\begin{bmatrix}\varepsilon_A(L)\\ \varepsilon_B(L)\end{bmatrix}=\exp\left(-\frac{2\phi^2}{\alpha}\right)\begin{bmatrix}\cos^2\phi\\ \sin^2\phi\end{bmatrix}. \tag{11}$$

The oscillation between the two modes show up at the output of the medium, and ϕ is the oscillation phase. A larger θ makes the oscillations more prominent. Thus, we set $\theta = \pi$ to give the maximum contrast or difference between two output probe fields at a small δ.

The number of oscillation cycles can be considerably increased with the storage and retrieval of SSL. The idea is based on our previous experience that the propagation time of the light pulses in the medium is equivalent to the storage time of the ones transformed into the atomic coherences ρ_1 and ρ_2. In Eq. (11) at $\theta = \pi$, the quantity $t_d \equiv \alpha\Gamma/(2\Omega^2)$, representing the SSL propagation delay time, determines the oscillation phase as

$$\phi=\frac{\alpha}{2}\frac{\delta\Gamma}{\Omega^2}=t_d\delta.$$

By storing SSL for a time t_s, the propagation time t_d is replaced by the storage time t_s in the oscillation phase of the SSL. Thus, the two retrieved probe fields are given by

$$\begin{bmatrix}\varepsilon_{A,\text{out}}\\ \varepsilon_{B,\text{out}}\end{bmatrix}=\exp\left(-\frac{t_s}{\tau_{\text{coh}}}\right)\begin{bmatrix}\cos^2\phi\\ \sin^2\phi\end{bmatrix},\ \text{where}\ \phi=t_s\delta\ \text{and}\ \tau_{\text{coh}}\ \text{is the coherence time.} \tag{12}$$

Because the storage time can be much longer than the propagation delay time, the oscillation is more prominent with the stored SSL. Furthermore, the decay factor of $\exp(-2\phi^2/\alpha)$ in Eq. (11) is the energy loss caused by the two-photon detuning during the propagation. This energy loss will not show up during the storage. On the other hand, the decay factor of $\exp(-t_s/\tau_{\text{coh}})$ in Eq. (12) is the energy loss caused by the decoherence process in the system, which can usually be much smaller than $\exp(-2\phi^2/\alpha)$. Although no derivation is provided here, we will demonstrate Eq. (12) with the experimental data and illustrate its physical picture later in Section 4.

3. EXPERIMENTAL SETUP

We carried out the experiment in cold ^{87}Rb atoms. The cigar-shaped cloud of cold atoms were produced by a magneto-optical trap (MOT)[54]. Typically, we can trap 1.0×10^9 atoms in the MOT as measured by the optical pumping method[55]. The temperature of the atoms was about 300 μK determined by the counter-propagating EIT scheme[56]. We employed the temporal dark MOT[57] to increase the optical density (OD) before performing each measurement. During the process of the dark MOT, the intensity of the repumping field was reduced from 1.1 mW/cm^2 to 4.4 μW/cm^2. In each measurement, we switched off the MOT to avoid the perturbation induced by the magnetic, trapping and repumping fields.

The four coupling fields Ω_{A1}, Ω_{A2}, Ω_{B1} and Ω_{B2} drove the transitions of $|5S_{1/2},F=2\rangle \rightarrow |5P_{1/2},F=2\rangle$, $|5S_{1/2},F=1\rangle \rightarrow |5P_{1/2},F=2\rangle$, $|5S_{1/2},F=2\rangle \rightarrow |5P_{3/2},F=2\rangle$ and $|5S_{1/2},F=1\rangle \rightarrow |5P_{3/2},F=2\rangle$, respectively, and had the σ+ polarization. We first employed an optical pumping field with the σ+ polarization, driving the transition from $|5S_{1/2},F=1\rangle$ to $|5P_{3/2},F=2\rangle$, together with the coupling fields Ω_{A1} and Ω_{B1}. These three fields made the ground Zeeman state of $|5S_{1/2},F=2,m=2\rangle$ (denoted as $|0\rangle$ in Fig. 1) become the only dark state in the system. All population was optically pumped into to $|0\rangle$. The two probe fields ε_A and ε_B drove the transitions of $|5S_{1/2},F=2\rangle \rightarrow |5P_{1/2},F=2\rangle$ and $|5S_{1/2},F=2\rangle \rightarrow |5P_{3/2},F=2\rangle$, respectively, and had the σ– polarization. Because all the ground Zeeman states other than $|0\rangle$ had no population, only the probe transitions of $|0\rangle \rightarrow |5P_{1/2},F=2,m=1\rangle$ (i.e. $|A\rangle$) and $|0\rangle \rightarrow |5P_{3/2},F=2,m=1\rangle$ (i.e. $|B\rangle$), and the coupling transitions of $|5S_{1/2},F=2,m=0\rangle$ (i.e. $|1\rangle$) $\rightarrow |A\rangle$ and $|5S_{1/2},F=1,m=0\rangle$ (i.e. $|2\rangle$) $\rightarrow |B\rangle$ were relevant. Consequently, the entire atom-light coupling scheme becomes a simple DT system as shown in Fig. 1, and all other states and transitions were irrelevant.

After all population was pumped into the ground state $|0\rangle$, we switched on Ω_{A2} and Ω_{B2}. As the four coupling fields for the SSL formation were present, we fired the probe pulse ε_A. Two photo multipliers (Hamamatsu PMT H6780-20 and H10720) were employed to detect the signals of the two output probe pulses ε_A and ε_B. Signals from the PMTs were sent to a digital oscilloscope (Agilent MSO6014A). Data were averaged 200 times by the oscilloscope before acquired by a computer. After the measurement was complete, we turned off the coupling fields and turned back on the MOT. The above measurement sequence was repeated every 0.15 s.

The important experimental parameters are listed below. The wavelength of ε_A, Ω_{A1} and Ω_{A2} is 795 nm and that of ε_B , Ω_{B1} and Ω_{B2} is 780 nm. The spontaneous decay rate (Γ) of the excited states $|A\rangle$ and $|B\rangle$ is about $2\pi\times6$ MHz. In the experimental system, the optical density (α) was 20 and the coherence time (τ_{coh}) was around 76 μs. We set all the coupling Rabi frequencies Ω_{A1}, Ω_{A2}, Ω_{B1} and Ω_{B2} to approximately 0.51Γ in the measurement. The input probe pulse had the Gaussian shape with an e^{-2} full width of 2.5 μs and a peak power of 15 nW, and its intensity was sufficiently weak to be considered as the perturbation such that Eqs. (1)-(3) are valid. We set the relative phase among the four coupling fields (θ) to π through the entire measurements. Other details can be found in Ref. 48.

4. RESULTS

4.1 Oscillation of Spinor Slow Light

We first demonstrated the oscillation phenomenon resulting from the SSL in the DT scheme as shown in Eq. (12). Only one probe pulse ε_A was sent to the input. As ε_A propagated through the atoms, the four coupling fields were constantly present. Then, we switched off the coupling fields to store the probe pulse in the atom cloud. After a storage time of t_s = 15 μs, we switched on the coupling fields and retrieved the probe pulse which now consisted of ε_A and ε_B. The retrieved energies of ε_A and ε_B were measured against the two-photon detuning δ or, equivalently, the oscillation phase ϕ. Figure 2 shows that the two signals of ε_A and ε_B oscillate alternatively; when one reaches minima the other becomes maxima and vice versa. The oscillation phenomenon behaves just like Eq. (12) which indicates

$$|\varepsilon_{A,\text{out}}|^2 \propto \cos^2\phi = [1+\cos(2\phi)]/2, \quad |\varepsilon_{B,\text{out}}|^2 \propto \sin^2\phi = [1-\cos(2\phi)]/2, \tag{13}$$

where $\phi = (t_s+t_d)\delta$, t_s (the storage time) = 15 μs and t_d (the propagation time) = 1 μs. Theoretically, the oscillation period is equal to π/(16 μs) = 2π×31 kHz. The best fit of the data shown in Fig. 2 determines the period being 2π×(30.8±0.1) kHz which is in agreement with the theoretical prediction.

We provide a physical picture to explain the result. As SSL is stored, there are two ground-state coherences ρ_1 and ρ_2 in the medium. The two-photon detunings δ and $-\delta$ make the precession frequencies of ρ_1 and ρ_2 different. At the retrieval, the phase difference between ρ_1 and ρ_2 determines how much ε_A and ε_B can be read out. This can be seen under the adiabatic condition as follows. At $\theta = \pi$, the Rabi frequencies of the four coupling fields with the same amplitude are equal to the values of $i\Omega$, Ω, Ω and $i\Omega$. As shown by Eq. (5) under $(\Gamma/2)\rho_A$ and $(\Gamma/2)\rho_B$ being negligible, the relation between $(\varepsilon_A, \varepsilon_B)$ and (ρ_1, ρ_2) is given by

$$\begin{bmatrix} \varepsilon_A \\ \varepsilon_B \end{bmatrix} = -\begin{bmatrix} i\Omega & \Omega \\ \Omega & i\Omega \end{bmatrix}\begin{bmatrix} \rho_1 \\ \rho_2 \end{bmatrix}. \tag{14}$$

Because only the probe ε_A is present at the input, $(\varepsilon_A, \varepsilon_B) = (\varepsilon_{A,\text{in}}, 0)$. Right after the storing process (denoted as $t = 0$), Eq. (14) results in

$$\rho_1(0) = (i/2)\varepsilon_{A,\text{in}}/\Omega, \quad \rho_2(0) = (-1/2)\varepsilon_{A,\text{in}}/\Omega. \tag{15}$$

The phases of $\rho_1(t)$ and $\rho_2(t)$ evolve with time during the storage. At $t = t_s$,

$$\rho_1(t_s) = e^{i\phi}\rho_1(0), \quad \rho_2(t_s) = e^{-i\phi}\rho_2(0), \tag{16}$$

where ϕ ($-\phi$) is the phase of ρ_1 (ρ_2) induced by the two-photon detuning. Right after the retrieving process, Eq. (14) gives

$$\varepsilon_{A,\text{out}} = [-i\rho_1(t_s) - \rho_2(t_s)]\Omega, \quad \varepsilon_{B,\text{out}} = [-\rho_1(t_s) - i\rho_2(t_s)]\Omega. \tag{17}$$

As $\phi = \pi/2$, with the help of Eqs. (15)-(17) we can see that only the probe ε_B is read out because

$$\varepsilon_{A,\text{out}} = \rho_1(0)+i\rho_2(0) = 0, \quad \varepsilon_{B,\text{out}} = -i\rho_1(0)-\rho_2(0) = \varepsilon_{A,\text{in}}.$$

As $\phi = \pi$, with the help of Eqs. (15)-(17) we can see that only the probe ε_A is read out because

$$\varepsilon_{A,\text{out}} = i\rho_1(0)+\rho_2(0) = -\varepsilon_{A,\text{in}}, \quad \varepsilon_{B,\text{out}} = \rho_1(0)+i\rho_2(0) = 0.$$

For other values of ϕ, both the probes ε_A and ε_B are read out as predicted by Eq. (12).

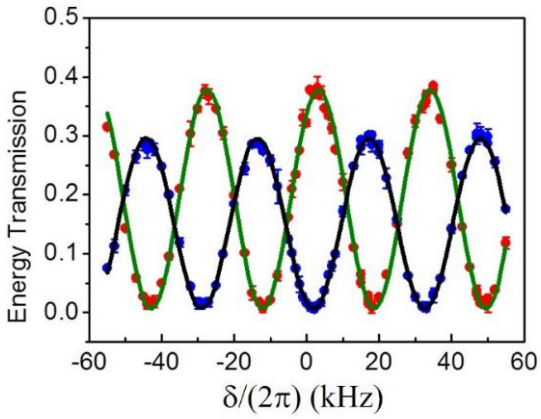

Figure 2. As only one probe pulse ε_A was present at the input, the stored and then retrieved energies of ε_A (red circles) and ε_B (blue circles) were measured against the two-photon detuning δ. The storage time is 15 μs. Green and purple lines are the best fits, determining the oscillation period equal to 2π×(30.8±0.1) kHz.

4.2 Spinor-Slow-Light Interferometer

The two signals, oscillating as functions of the detuning δ or equivalently the phase difference ϕ as shown in Fig. 2, are similar to those of an interferometer. This suggests that one can use SSL as an interferometer to precisely determine the two-photon detuning δ. The coherence time in the experiment was about 76 μs. Using the sufficiently long coherence time, we experimentally demonstrated the idea of SSL interferometer with two measurement series. In the first measurement series, we set δ to $2\pi\times10$ kHz, and the measured data are shown in Fig. 3(a). In the second measurement series, we set δ to $2\pi\times20$ kHz, and the measured data are shown in Fig. 3(b). Note that the difference of two values of δ can be set much more precisely than their absolute values. The difference in δ of the two measurement series was $2\pi\times10.0$ kHz. The retrieved ε_A and ε_B energies were taken against the storage time as shown in the figures. The best fits of the data determine the oscillation periods (T_s) being 49.9±0.3 μs in Fig. 3(a) and being 25.3±0.1 μs in Fig. 3(b). According to Eq. (12), we have $\delta = \pi/T_s$, which gives the difference in δ equal to $2\pi\times9.7$ kHz. The measured value of the difference is consistent with the actual one, showing that the SSL interferometer can be used to determine the detuning δ induced by light shifts, Zeeman shifts, etc. The frequency precision demonstrated here is of the order of 100 Hz under a storage time close to 100 μs. In principle, a longer storage time allows to determine the frequency more precisely. An optical dipole trap can be employed to confine cold atoms, leading to the storage time of about 1 s for stored light[15]. Extrapolating from our data, a storage time of 1 s may result in a frequency precision of 0.01 Hz for the SSL interferometer.

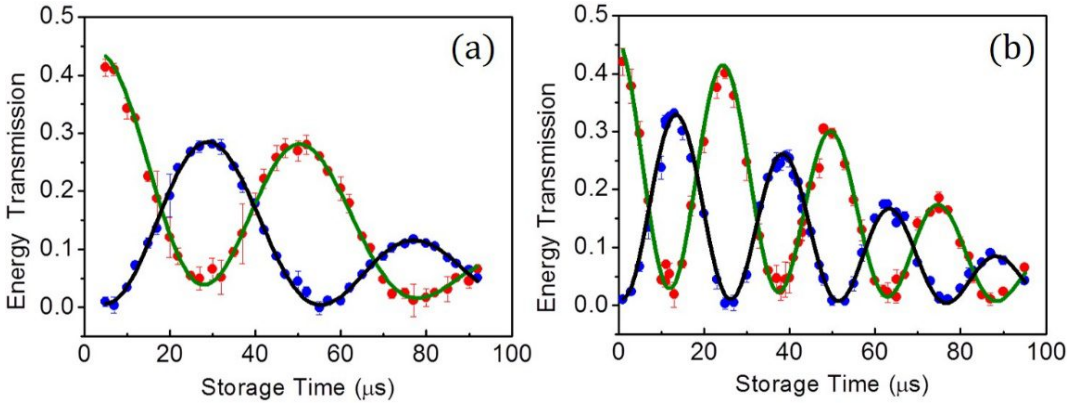

Figure 3. As only one probe pulse ε_A was present at the input, the stored and then retrieved energies of ε_A (red circles) and ε_B (blue circles) were measured against the storage time. The two-photon detuning δ was set to approximately $2\pi\times10$ kHz in (a) and approximately $2\pi\times20$ kHz in (b). The difference of the two values of δ was precisely equal to $2\pi\times10.0$ kHz. The best fit in (a) determines the oscillation period equal to 49.9±0.3 μs and the decay time constant equal to 76.8±1.2 μs. The best fit in (b) determines the oscillation period equal to 25.3±0.1 μs, and the decay time constant equal to 75.8±1.5 μs.

4.3 Two-Color Qubits

Single-photon SSL can be considered as a two-color qubit whose wave function is the superposition state of two frequency modes given by

$$|\psi\rangle = \cos\phi|1_{\omega_A}, 0_{\omega_A}\rangle + \sin\phi\,|0_{\omega_A}, 1_{\omega_A}\rangle. \tag{18}$$

Photons in two-color quantum states are inert to birefringent materials, e.g. optical fibers, being a desirable feature of the information carrier in long-distance quantum communication. The two-color qubit in our case has the frequency mode ω_A corresponding to the wavelength of 795 nm and the frequency mode ω_B corresponding to the wavelength of 780 nm. One is able to produce such qubit by sending a single photon with the wavelength of either 795 or 780 nm to the DT system. The oscillation behavior shown in Figs. 3(a) and 3(b) can be considered as the Rabi oscillation in a two-level system, the precession of a spin, or the state rotation of a qubit. The two-photon detuning for SSL or two-color qubits here is in analogy with the magnetic field for spins.

The DT system can employed as the quantum memory. To see this, we sent both ε_A and ε_B pulses to the medium and set $\delta = 0$ during the storage. The temporal profiles of the two retrieved pulses at different values of $(\cos\phi/\sin\phi)^2$ = 1.5, 0.9 and 0.5 are shown in Figs. 4(a)-4(c), respectively. In each figure, the pulse shapes of the readout ε_A and ε_B after the storage time of 3 μs are very close to those after the storage time of 33 μs. In all figures, the energy ratios after the storage time of 3 μs are also nearly the same as those after the storage time of 33 μs. Furthermore, one can also apply a two-photon detuning δ during the storage period to change the values of $\cos\phi$ and $\sin\phi$ in Eq. (18). The detuning is made by the Zeeman or a.c. Stark shift induced by a pulse of magnetic field or by a far detuned microwave or laser pulse. The amount of the change is controlled by the product of the detuning and pulse duration. An example of rotating $(\varepsilon_A, \varepsilon_B) = (1, 0)$ to $(\varepsilon_A, \varepsilon_B) = (\cos\phi, \sin\phi)$ has been demonstrated by the data in Fig. 2. Our demonstrations of memory and rotator were done with classical light. Nevertheless, due to quantum nature of the EIT effect the results suggest that the DT scheme can lead to the applications of quantum memory and quantum rotator for two-color qubits.

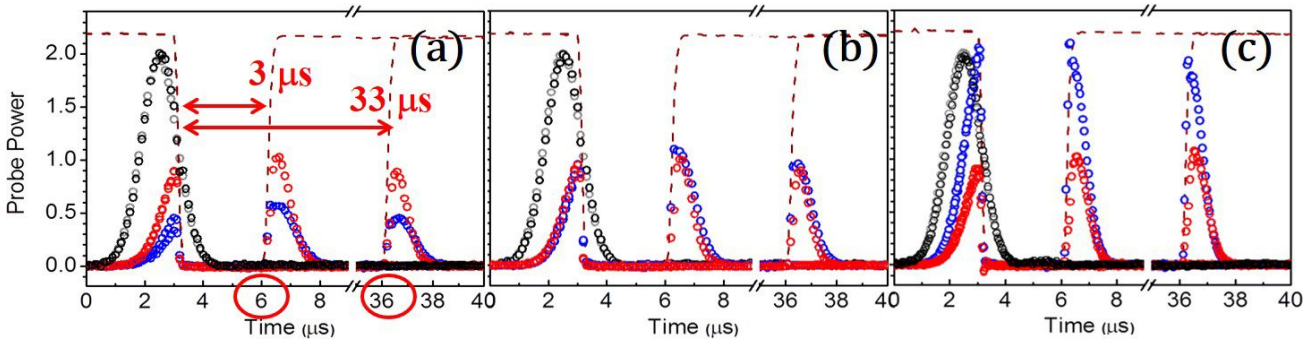

Figure 4. Storage and retrieval of SSL and the detuning $\delta = 0$ during the storage period. Black and gray circles are the input ε_A and ε_B pulses scaled up or down by the factors of 0.92 and 0.92 in (a), 1.29 and 0.73 in (b) and 1.73 and 0.40 in (c). Red and blue circles are the two retrieved ε_A and ε_B pulses after storage times of 3 and 33 μs. Energy ratios of the two retrieved pulses after the storage times of 3 and 33 μs are 1.5 and 1.5 in (a), 0.84 and 0.92 in (b) and 0.55 and 0.52 in (c).

5. CONCLUSION

We observed two-component or spinor slow light (SSL) in the double tripod (DT) system as demonstrated by the oscillation between its two components of the wavelengths of 780 nm and 795 nm. The data of the light-storage DT scheme were used to determine the two-photon detuning with the satisfactory accuracy and precision, suggesting the application of the SSL interferometer for precision measurements. Single-photon SSL can be considered as a two-color qubit. As a proof-of-principle experiment, we showed that the DT scheme can be employed as the quantum memory and quantum rotator for the two-color qubits. Furthermore, the SSL may lead to interesting physics such as Dirac particles[44], Klein tunneling[45] and spinor Bose-Einstein condensation of dark-state polaritons[19]. This work opens a new avenue in the slow light research.

REFERENCES

[1] Harris, S. E., "Electromagnetically induced transparency," Phys. Today 50, 36–42 (1997).
[2] Lukin, M. D., "Colloquium: trapping and manipulating photon states in atomic ensembles," Rev. Mod. Phys. 75, 457–472 (2003).
[3] Fleischhauer, M., Imamoglu, A., and Marangos, J. P., "Electromagnetically induced transparency: optics in coherent media," Rev. Mod. Phys. 77, 633–673 (2005).
[4] Hau, L. V., Harris, S. E., Dutton, Z., and Behroozi, C. H., "Light speed reduction to 17 meters per second in an ultracold atomic gas," Nature (London) 397, 594–598 (1999).
[5] Kash, M. M. *et al*., "Ultraslow Group Velocity and Enhanced Nonlinear Optical Effects in a Coherently Driven Hot Atomic Gas," Phys. Rev. Lett. 82, 5229–5232 (1999).
[6] Novikova, I., Phillips, D. F., and Walsworth, R. L., "Slow Light with Integrated Gain and Large Pulse Delay," Phys. Rev. Lett. 99, 173604 (2007).

[7] Krauss, T. F., "Why do we need slow light?" Nat. Photon. 2, 448–450 (2008).
[8] Khurgin, J. B., "Slow light in various media: a tutorial," Adv. Opt. Photon. 2, 287–318 (2010).
[9] Fleischhauer, M. and Lukin, M. D., "Dark-State Polaritons in Electromagnetically Induced Transparency," Phys. Rev. Lett. 84, 5094–5097 (2000).
[10] Liu, C., Dutton, Z., Behroozi, C. H., and Hau, L. V., "Observation of coherent optical information storage in an atomic medium using halted light pulses," Nature 409, 490–493 (2001).
[11] Phillips, D. F., Fleischhauer, A., Mair, A., Walsworth, R. L., and Lukin, M. D., "Storage of Light in Atomic Vapor," Phys. Rev. Lett. 86, 783–786 (2001).
[12] Juzeliūnas, G. and Carmichael, H. J., "Systematic formulation of slow polaritons in atomic gases," Phys. Rev. A 65, 021601(R) (2002).
[13] Longdell, J. J., Fraval, E., Sellars, M. J., and Manson, N. B., "Stopped Light with Storage Times Greater than One Second Using Electromagnetically Induced Transparency in a Solid," Phys. Rev. Lett. 95, 063601 (2005).
[14] Schnorrberger, U. *et al*., "Electromagnetically Induced Transparency and Light Storage in an Atomic Mott Insulator," Phys. Rev. Lett. 103, 033003 (2009).
[15] Zhang, R., Garner, S. R., and Hau, L. V., "Creation of Long-Term Coherent Optical Memory via Controlled Nonlinear Interactions in Bose-Einstein Condensates," Phys. Rev. Lett. 103, 233602 (2009).
[16] Chen, Y.-H. *et al*., "Coherent Optical Memory with High Storage Efficiency and Large Fractional Delay," Phys. Rev. Lett. 110, 083601 (2013).
[17] Heinze, G., Hubrich, C., and Hoffman, T., "Stopped Light and Image Storage by Electromagnetically Induced Transparency up to the Regime of One Minute," Phys. Rev. Lett. 111, 033601 (2013).
[18] Bajcsy, M., Zibrov, A. S., and Lukin, M. D., "Stationary pulses of light in an atomic medium," Nature 426, 638–641 (2003).
[19] Fleischhauer, M., Otterbach, J., and Unanyan, R. G., "Bose-Einstein Condensation of Stationary-Light Polaritons," Phys. Rev. Lett. 101, 163601 (2008).
[20] Lin, Y. W. *et al*., "Stationary Light Pulses in Cold Atomic Media and without Bragg Gratings," Phys. Rev. Lett. 102, 213601 (2009).
[21] Otterbach, J., Ruseckas, J., Unanyan, R. G., Juzeliūnas, G., and Fleischhauer, M., "Effective magnetic fields for stationary light," Phys. Rev. Lett. 104, 033903 (2010).
[22] Schmidt, H. and Imamoglu, A., "Giant Kerr nonlinearities obtained by electromagnetically induced transparency," Opt. Lett. 21, 1936–1938 (1996).
[23] Harris, S. E. and Yamamoto, Y., "Photon Switching by Quantum Interference," Phys. Rev. Lett. 81, 3611–3614 (1998).
[24] Balić, V., Braje, D. A., Kolchin, P., Yin, G. Y., and Harris, S. E., "Generation of Paired Photons with Controllable Waveforms," Phys. Rev. Lett. 94, 183601 (2005).
[25] Eisaman, M. D. *et al*., "Electromagnetically induced transparency with tunable single-photon pulses," Nature 438, 837–841 (2005).
[26] Wang, Z. B., Marzlin, K.-P., and Sanders, B. C., "Large Cross-Phase Modulation between Slow Copropagating Weak Pulses in ^{87}Rb," Phys. Rev. Lett. 97, 063901 (2006).
[27] Wang, C. Y. *et al*., "Low-light-level all-optical switching," Opt. Lett. 31, 2350 (2006).
[28] Belthangady, C. *et al*., "Hiding Single Photons with Spread Spectrum Technology," Phys. Rev. Lett. 104, 223601 (2010).
[29] Shiau, B. W., Wu, M. C., Lin, C. C., and Chen, Y. C., "Low-Light-Level Cross-Phase Modulation with Double Slow Light Pulses," Phys. Rev. Lett. 106, 193006 (2011).
[30] Chen, Y. H. *et al*., "Demonstration of the Interaction between Two Stopped Light Pulses," Phys. Rev. Lett. 108, 173603 (2012).
[31] Peyronel, T. *et al*., "Quantum nonlinear optics with single photons enabled by strongly interacting atoms," Nature 488, 57–60 (2012).
[32] Venkataraman, V., Saha, K., and Gaeta, A. L., "Phase modulation at the few-photon level for weak-nonlinearity-based quantum computing," Nat. Photon. 7, 138–141 (2013).
[33] Chen, W. *et al*., "All-optical switch and transistor gated by one stored photon," Science 341, 768–770 (2013).
[34] Maxwell, D. *et al*., "Storage and Control of Optical Photons Using Rydberg Polaritons," Phys. Rev. Lett. 110, 103001 (2013).
[35] Baur, S., Tiarks, D., Rempe, G., and Dürr, S., "Single-Photon Switch Based on Rydberg Blockade," Phys. Rev. Lett. 112, 073901 (2014).

[36] Duan, L. M., Lukin, M. D., Cirac, J. I., and Zoller, P., "Long-distance quantum communication with atomic ensembles and linear optics," Nature 414, 413–418 (2001).
[37] Chanelière, T. *et al*., "Storage and retrieval of single photons transmitted between remote quantum memories," Nature 438, 833–836 (2005).
[38] Chen, Y. F., Liu, Y. C., Tsai, Z. H., Wang, S. H., and Yu, I. A., "Beat-note interferometer for direct phase measurement of photonic information," Phys. Rev. A 72, 033812 (2005).
[39] Chen, Y. F., Wang, S. H., Wang, C. Y., and Yu, I. A., "Manipulating the retrieved width of stored light pulses," Phys. Rev. A 72, 053803 (2005).
[40] Chen, Y. F., Kuan, P. C., Wang, S. H., Wang, C. Y., and Yu, I. A., "Manipulating the retrieved frequency and polarization of stored light pulses," Opt. Lett. 31, 3511 (2006).
[41] Choi, K. S., Deng, H., Laurat, J., and Kimble, H. J., "Mapping photonic entanglement into and out of a quantum memory," Nature 452, 67–71 (2008).
[42] Zhao, B. *et al*., "A millisecond quantum memory for scalable quantum networks," Nat. Phys. 5, 95–99 (2009).
[43] Zhou, S. *et al*., "Optimal storage and retrieval of single-photon waveforms," Opt. Express 20, 24124–24131 (2012).
[44] Unanyan, R. G. *et al*., "Spinor Slow-Light and Dirac Particles with Variable Mass," Phys. Rev. Lett. 105, 173603 (2010).
[45] Ruseckas, J. *et al*., "Photonic-band-gap properties for two-component slow light," Phys. Rev. A 83, 063811 (2011).
[46] Ruseckas, J., Kudriašov, V., Yu, I. A., and Juzeliūnas, G., "Transfer of orbital angular momentum of light using two-component slow light," Phys. Rev. A 87, 053840 (2013).
[47] Bao, Q. Q. *et al*., "Coherent generation and dynamic manipulation of double stationary light pulses in a five-level double-tripod system of cold atoms," Phys. Rev. A 84, 063812 (2011).
[48] Lee, M. J. *et al*., "Experimental demonstration of spinor slow light," Nature Commun. 5, 5542 (2014).
[49] Petrosyan, D. and Malakyan, Y. P., "Magneto-optical rotation and cross-phase modulation via coherently driven four-level atoms in a tripod configuration," Phys. Rev. A 70, 023822 (2004).
[50] Raczyński, A., Zaremba, J., and Zielińska-Kaniasty, S., "Beam splitting and Hong-Ou-Mandel interference for stored light," Phys. Rev. A 75, 013810 (2007).
[51] Wang, H. H. *et al*., "Slowing and storage of double light pulses in a Pr^{3+}:Y_2SiO_5 crystal," Opt. Lett. 34, 2596–2598 (2009).
[52] Karpa, L., Vewinger, F., and Weitz, M., "Resonance Beating of Light Stored Using Atomic Spinor Polaritons," Phys. Rev. Lett. 101, 170406 (2008).
[53] Ruseckas, J., Mekys, A., and Juzeliūnas, G., "Slow polaritons with orbital angular momentum in atomic gases," Phys. Rev. A 83, 023812 (2011).
[54] Lin, Y. W., Chou, H. C., Dwivedi, P. P., Chen, Y. C., and Yu, I. A., "Using a pair of rectangular coils in the MOT for the production of cold atom clouds with large optical density," Opt. Express 16, 3753-3761 (2008).
[55] Chen, Y. C., Liao, Y. A., Hsu, L., and Yu, I. A., "Simple technique for directly and accurately measuring the number of atoms in a magneto-optical trap," Phys. Rev. A 64, 031401(R) (2001).
[56] Su, S.W., Chen, Y. H., Gou, S. C., Horng, T. L., and Yu, I. A., "Dynamics of slow light and light storage in a Doppler-broadened electromagnetically-induced-transparency medium: A numerical approach," Phys. Rev. A 83, 013827 (2011).
[57] Ketterle, W., Davis, K. B., Joffe, M. A., Martin, A., and Pritchard, D. E., "High densities of cold atoms in a dark spontaneous-force optical trap," Phys. Rev. Lett. 70, 2253-2256 (1993).